

Molecular Simulation of Cross-Nucleation between Polymorphs

Caroline Desgranges and Jerome Delhommelle*

Department of Chemical Engineering, University of South Carolina, 301 Main Street South, Columbia, South Carolina 29201

Received: November 6, 2006; In Final Form: December 6, 2006

Recent experiments report that an early nucleating crystalline structure (or polymorph) may nucleate another polymorph. We use molecular dynamics simulations to model this phenomenon known as cross-nucleation. We study the onset of crystallization in a liquid of Lennard-Jones particles cooled at a temperature 22% below the melting temperature. We show that growth proceeds through the successive cross-nucleation of the metastable hexagonal close-packed (hcp) polymorph on the stable face-centered cubic (fcc) polymorph and of the stable fcc polymorph on the metastable hcp polymorph. This finding is in agreement with the experimental results which demonstrated that the cross-nucleation of a stable polymorph on a metastable polymorph is just as likely as the cross-nucleation of a metastable polymorph on a stable polymorph. We then extend our findings established in the case of the homogeneous crystal nucleation to a situation of practical interest, i.e., when a seed of the stable polymorph is used. By studying the crystal growth from the (111) plane of a perfect fcc crystal, we show that, again, growth proceeds through the cross-nucleation of the hcp and fcc structures.

1. Introduction

Polymorphism is the ability of a molecule to crystallize in different structures. This phenomenon is important for many applications since polymorphs often exhibit very different physical properties. For instance, different polymorphs of the same drug may have different dissolution rates and solubilities. Since these two properties play a major role in determining the bioavailability of a drug substance, it is especially important for the pharmaceutical industry to understand and control polymorphism.¹ However, the control of crystallization in a polymorphic system still remains an unsolved problem. Polymorphs may suddenly appear or disappear.² The shortage of the AIDS drug Ritonavir resulted from the sudden formation of a new polymorph.³ In some cases, the control of polymorphism is extremely challenging as more than one polymorph form at the same time (this phenomenon is known as concomitant polymorphism).⁴

Several mechanisms were proposed to account for concomitant polymorphism. The concomitant formation of more than one polymorph may be understood in terms of competing processes of homogeneous nucleation of different polymorphs.⁵ Alternatively, it may result from the solvent-mediated conversion of one polymorph into another.⁶ A third mechanism, known as cross-nucleation, was recently discovered by Yu.⁷ In his experimental study of the crystallization of D-sorbitol and D-mannitol, Yu showed that an early nucleating polymorph may cross-nucleate another polymorph instead of consuming the entire liquid. Cross-nucleation since has been observed in several experimental studies.^{8–11} It is an important phenomenon for both practical and fundamental reasons. In industrial crystallization, seeding, i.e., the introduction of small crystallites of a given polymorph in a supersaturated solution, is the technique used to control polymorphism. If cross-nucleation takes place in a polymorphic system, seeding becomes ineffective. From a fundamental point of view, cross-nucleation is a new phenom-

enon. It is not taken into account in current models or theories of nucleation and crystallization in polymorphic systems. For instance, Ostwald's rule of stages states that the least stable polymorph should form first and then should convert into the second least stable polymorph and so on to the most stable.¹² Since a metastable polymorph is sometimes observed to cross-nucleate on a stable polymorph,⁹ Ostwald's rule of stages cannot be used to understand the phenomenon of cross-nucleation. Other models,^{5,13} which assume that polymorphs nucleate and grow independently from each other, are also unable to account for cross-nucleation.

In a recent communication,¹⁴ we proposed to use molecular dynamics (MD) simulations to model cross-nucleation and provide insight into the molecular mechanisms underlying this phenomenon. We studied the onset of crystallization in a liquid of Lennard-Jones particles cooled at a temperature 22% below the melting temperature.¹⁵ Under these thermodynamic conditions, the stable polymorph is the face-centered cubic (fcc) structure.^{15–17} There are also two metastable polymorphs: the hexagonal close-packed (hcp) structure, whose free energy is very close to that of fcc,¹⁷ and the body-centered cubic (bcc) structure of higher free energy. We simulated the two mechanistic steps of crystallization, i.e., the nucleation and growth steps. During the growth step, we observed the cross-nucleation of the metastable hcp polymorph on post-critical crystallites whose structure was predominantly that of the fcc structure.

The aim of this work is twofold. First, we pursue our previous work by studying the growth of a critical nucleus in a much larger system. This allows us to model the growth step well beyond the first cross-nucleation observed in our previous work.¹⁴ We show that growth proceeds through the successive cross-nucleation of (i) the metastable hcp polymorph on the stable fcc polymorph and (ii) the stable fcc polymorph on the metastable hcp polymorph. This result is in excellent agreement with the experimental results of Yu and co-workers.^{7,9} They showed that cross-nucleation is a kinetic phenomenon and that the cross-nucleation of a stable polymorph on a metastable

* Address correspondence to this author. E-mail: delhomm@engr.sc.edu.

polymorph is just as likely as the cross-nucleation of a metastable polymorph on a stable polymorph. Second, we extend our findings established in the case of a crystallite obtained by homogeneous nucleation to a situation of practical interest, i.e., when a seed of the stable polymorph is used. For this purpose, we study the crystal growth from the (111) plane of a perfect fcc crystal and show that, again, growth proceeds through cross-nucleation of the hcp and fcc structures.

This paper is organized as follows. We first present the simulation methods used to simulate the two mechanistic steps of crystal nucleation and growth. We then explain how we assign a specific structure for each Lennard-Jones particle of the system. We also detail how we carry out MD simulations of the growth from the (111) plane of a perfect fcc crystal. We then discuss the results obtained for both types of simulation and draw our conclusions.

2. Simulation Methods

We carry out two different types of MD simulations corresponding to the two mechanistic steps of nucleation and growth.

First, we simulate the formation of a critical nucleus. We study a supercooled liquid of Lennard-Jones particles at a reduced pressure $P = 5.68$ and a reduced temperature $T = 0.86$ (a temperature 22% below the melting point).¹⁵ Throughout this paper, we use the conventional system of reduced units for the Lennard-Jones system.¹⁸ For a degree of supercooling of 22%, nucleation is an activated process associated with a large free energy barrier of formation. We therefore used the umbrella sampling technique¹⁹ to study the formation of a crystal nucleus. We perform MD simulations together with an umbrella sampling bias potential¹⁹ on systems containing 4000 Lennard-Jones particles. The bias potential allows the system to overcome the free energy barrier of nucleation.^{20–23} It imposes a fixed value of the global order parameter Q_6 to the system²⁴ (this bias potential does not favor the formation of a specific polymorph since Q_6 takes similar values for the fcc, hcp, and bcc polymorphs). By gradually increasing the imposed value for Q_6 , we are able to grow a crystal nucleus.

Once we have formed the critical nucleus, we study its evolution in the absence of the bias potential according to the method used in our previous work on this system.¹⁴ In this work, we embed the system of 4000 particles containing a critical nucleus in a supercooled liquid of 96 000 particles and obtain a system of overall 100 000 particles. We then equilibrate the new system according to two successive steps: (i) the central region of 4000 particles is kept fixed and the rest of the system follows a normal NPT molecular dynamics trajectory and (ii) we apply the umbrella sampling bias potential to the central subsystem of 4000 particles and integrate the NPT equations of motion for the whole system (this preserves the crystalline embryo). Every 10 time units, we store a configuration of the system. The stored configurations were then used as starting points of unbiased NPT molecular dynamics simulations (i.e., simulations for which we have switched off the umbrella sampling potential). This allows us to study the free evolution of the critical nucleus at fixed temperature and pressure. We emphasize that in our previous work on the Lennard-Jones system, we generated 15 free MD trajectories. We observed the dissolution of the nucleus in the surrounding liquid for 7 of them and the growth of the nucleus in the remaining 8 MD trajectories. The 7:8 ratio, close to the ideal 5:5 ratio, expected for a critical nucleus, demonstrated that the crystal nuclei we have formed are genuine critical nuclei. In this work, given the overall size of the system, we only study one MD trajectory leading to the growth of the critical nucleus.

Throughout the nucleation and growth steps, we need to identify the structural identity (fcc, hcp, or bcc) of each particle. We first briefly outline how we distinguish between solid-like and liquid-like particles (this is done according to the method proposed by ten Wolde and co-workers²¹). For a given particle i , we use the local orientational order parameters $\bar{q}_{lm}(i)$ ($m = -l, \dots, l$) which are expansions in spherical harmonic of the bond vectors between nearest neighbors i and j . They are defined according to

$$\bar{q}_{lm}(i) = \frac{\sum_j Y_{lm}(\hat{\mathbf{r}}_{ij}) \alpha(r_{ij})}{\sum_j \alpha(r_{ij})} \quad (1)$$

where $Y_{lm}(\hat{\mathbf{r}}_{ij})$ is a spherical harmonics, and $\alpha(r_{ij})$ a weight function ($\alpha(r_{ij}) = (r_{ij} - r_q)^2$ for $r_{ij} < r_q$ and $\alpha(r_{ij}) = 0$ elsewhere). j denotes a particle that belongs to the first coordination shell of particle i and \mathbf{r}_{ij} the vector joining the centers of mass of particles i and j (r_{ij} stands for the norm of this vector and $\hat{\mathbf{r}}_{ij}$ the corresponding unit vector). $r_q = 1.4\sigma$ corresponds to the first minimum of $g(r)$ in the fcc crystal of the Lennard-Jones.

We now define the normalized 13-dimensional ($m = -6, \dots, 6$) complex vector $q_6(i)$ of components $\bar{q}_{6m}(i)$ as

$$\bar{q}_{6m}(i) = \frac{\bar{q}_{6m}(i)}{(\sum_{m=-6}^6 |\bar{q}_{6m}(i)|^2)^{1/2}} \quad (2)$$

The dot product of the vectors \mathbf{q}_6 of two neighboring particles i and j is

$$\mathbf{q}_6(i) \cdot \mathbf{q}_6(j) = \sum_{m=-6}^6 \bar{q}_{6m}(i) \bar{q}_{6m}^*(j) \quad (3)$$

Two particles are considered to be connected if $\mathbf{q}_6(i) \cdot \mathbf{q}_6(j)$ is larger than 0.5, i.e., if their local order parameters are correlated. We find that the number of connections per particle rarely exceeds 8 in the liquid phase (less than 1% are identified as solid-like) and is seldom below 8 in both solid phases. A particle connected to at least 8 particles of its first neighbors is considered as solid-like and liquid-like otherwise.

We now explain how we distinguish between fcc-like, bcc-like, and hcp-like particles. The order parameters considered in this analysis (i.e., q_4 and \hat{w}_4) are defined from the local order parameters $\bar{q}_{lm}(i)$ as

$$q_l(i) = \left[\frac{4\pi}{2l+1} \sum_{m=-l}^l |\bar{q}_{lm}(i)|^2 \right]^{1/2} \quad (4)$$

$$\hat{w}_l(i) = \frac{w_l(i)}{[\sum_{m=-l}^l |\bar{q}_{lm}(i)|^2]^{3/2}} \quad (5)$$

where

$$\hat{w}_l(i) = \sum_{\substack{m_1, m_2, m_3 \\ m_1+m_2+m_3=0}} \begin{pmatrix} l & l & l \\ m_1 & m_2 & m_3 \end{pmatrix} \times \bar{q}_{lm_1}(i) \bar{q}_{lm_2}(i) \bar{q}_{lm_3}(i) \quad (6)$$

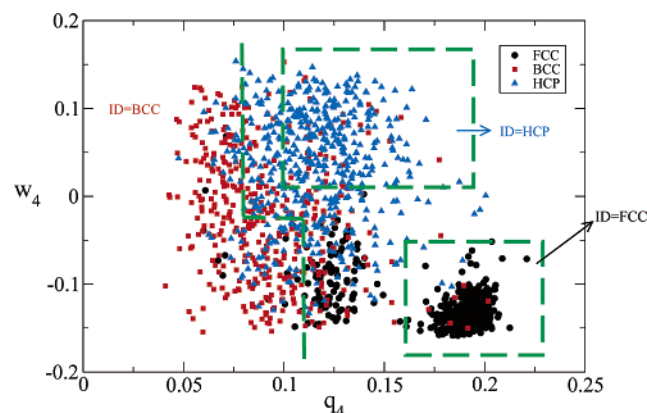


Figure 1. Summary of the rules used to determine whether a Lennard-Jones particle is fcc-like, bcc-like, or hcp-like.

We compute the distributions for the two local order parameters q_4 and w_4 for the three crystalline structures fcc, bcc, and hcp at the temperature of 0.8625. On the basis of these distributions, we identify a particle i as follows: fcc-like if $q_4(i) > 0.16$ and $w_4(i) < -0.05$; bcc-like if $q_4(i) < 0.08$ or if $q_4(i) < 0.11$ and $w_4(i) < -0.025$; and hcp-like if $q_4(i) > 0.1$ and $w_4(i) > 0.04$.

We sum up these rules in Figure 1. As shown in Figure 1, we did not try to assign a specific structure to a particle where there was a significant overlap between the distributions of local order parameters for two different structures. We therefore made a conservative choice. This is because we prefer being positive on the structural identity of a given particle and leave the identity of some particles as undetermined. In particular, Figure 1 also shows that there is almost no overlap between the fcc and hcp domains as defined by our rules. This is especially important since this allows us to determine without any ambiguity that cross-nucleation takes place between the fcc and hcp structures. We find this analysis satisfactory since it allows us to identify 80% of the structure inside the crystal nucleus.

We extend our findings established in the case of the homogeneous crystal nucleation to a situation of practical interest, i.e., when a seed of the stable polymorph is used. For this purpose, we study the crystal growth from the (111) plane of a perfect fcc crystal. We first generate a perfect (111) fcc crystal lattice composed of $N_x \times N_y \times N_z = 18 \times 20 \times 54 = 19\,440$ particles. We equilibrate this system at $P = 5.68$ and $T = 0.5$ for 10 time units. Then, we freeze 9 layers (3240 particles) along the z axis and melt the rest of the system at $P = 5.68$ and $T = 1.5$ (well above the melting temperature of 1.1¹⁵) for 20 time units. Then, every 10 time units, we store a configuration of the system (we store a total of 10 configurations). Each stored configuration is then used as a starting point for a growth trajectory in which we set the temperature to $T = 0.86$, let the whole system evolve, and monitor the increase in the number of fcc, bcc, and hcp particles with time.

3. Results and Discussion

We briefly outline the results obtained for the nucleation step. Our findings are in accord with the results of previous work.²¹ During the nucleation step, the system follows Ostwalds rule of stages. Nucleation first proceeds into the bcc metastable polymorph with the formation of small bcc nuclei. As the nucleus grows, it steadily evolves toward the stable fcc structure (a recent analysis by Trudu et al.²⁵ demonstrates that nucleation in a Lennard-Jones system is a two-step process). The critical nucleus contains 339 ± 45 particles and can be described as a

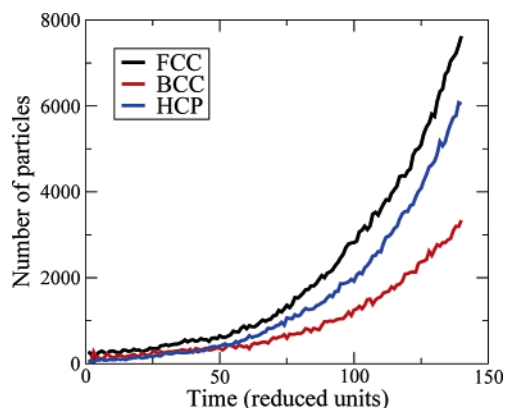


Figure 2. Evolution of the number of fcc-like, bcc-like, and hcp-like particles during the growth of the crystal nucleus.

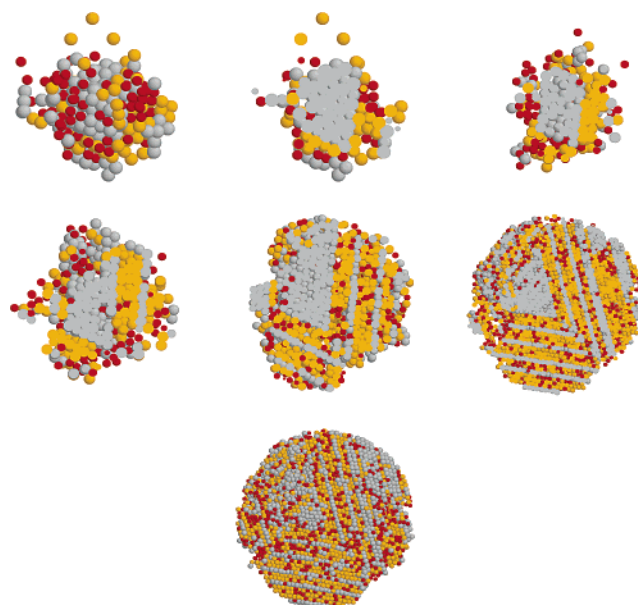


Figure 3. Growth of a Lennard-Jones crystallite: outside view and cross-section of a critical nucleus ($t = 0$ indicates when the bias potential is switched off and the nucleus starts to evolve freely); cross-section at $t = 20, 40$, and 80 ; cross-section and outside view at the end of the MD trajectory ($t = 140$). Gray: fcc-like particles; yellow: hcp-like particles; and red: bcc-like particles.

fcc core wetted by bcc particles (the free energy barrier of nucleation is of $(22.6 \pm 1.0)k_B T$). The number of hcp particles is still negligible at this point.

We now present the results obtained during the growth step. Throughout this step, we monitor the increases in the number of fcc (N_{fcc}), hcp (N_{hcp}), and bcc (N_{bcc}) particles. The results are plotted in Figure 2. We also provide snapshots of the post-critical nuclei in Figure 3. In Figure 2, $t = 0$ indicates the time at which the umbrella sampling potential is switched off (as detailed in the previous section, our method ensures that at $t = 0$, the crystal nucleus is a genuine critical nucleus). At first ($t < 5$), when the crystal nucleus is still close to the critical nucleus, we observe significant fluctuations in the size and structure of the nucleus. The structure of the crystal nucleus is successively dominated by the fcc structure (at $t = 1$, we have 257 fcc particles for 44 bcc particles), by the bcc structure (at $t = 3$, $N_{\text{fcc}} = 71$ and $N_{\text{bcc}} = 250$), and finally by the fcc structure again (at $t = 4$, $N_{\text{fcc}} = 197$ and $N_{\text{bcc}} = 127$). This is in agreement with the findings of Moroni et al.,²⁶ who showed that there is a significant interplay between the size and structure of critical nuclei in the Lennard-Jones system.

Then, for $5 < t < 15$, the nucleus grows very slowly. N_{fcc} slowly increases from 244 at $t = 5$ to 306 for $t = 15$, while N_{bcc} from 125 ($t = 5$) to 154 ($t = 15$) and N_{hcp} from 74 ($t = 5$) to 86 ($t = 15$) remain almost constant. From the snapshots, we can infer the following mechanism of growth. The crystal nucleus has a fcc core, wetted by bcc and hcp particles. The bcc and hcp particles progressively convert into fcc particles and contribute to the growth of the fcc core.

Around $t = 15$, N_{hcp} starts to grow at a faster rate. This corresponds to the cross-nucleation of a cluster of hcp particles on the structurally compatible (111) plane of the fcc core of the nucleus. This can be clearly seen on the cross section of the nucleus at $t = 20$ plotted in Figure 3, which shows that several layers of hcp form on the nucleus (see the right of the snapshot).

From that point on, N_{hcp} increases at a much faster rate than N_{bcc} and at a similar rate to that observed for N_{fcc} . N_{hcp} eventually becomes larger than N_{bcc} at $t = 46$. The core of the nucleus is now mainly composed of fcc and hcp particles. N_{fcc} and N_{hcp} increase faster than N_{bcc} since they both grow with the volume of the nucleus. On the other hand, N_{bcc} increases with the surface of the nucleus and hence at a slower rate. Throughout the MD trajectory, N_{bcc} retains a steady growth rate, indicating that the bcc particles always play the same role. Bcc particles are scattered on the surface of the fcc and hcp crystals before converting to either fcc or hcp. We do not observe any cross-nucleation of the least stable polymorph bcc on any of the hcp or fcc crystals.

This result confirms our previous report of cross-nucleation between polymorphs of the Lennard-Jones system.¹⁴ Like any nucleation event, cross-nucleation is an activated process. The fact that we observe this phenomenon on several MD trajectories indicates that the free energy barrier of cross-nucleation is much lower than that of homogeneous nucleation and can be easily overcome by the collective fluctuations in the fluid.^{27,28} This is in accord with what one would expect for any heterogeneous nucleation event.²⁹

One of the objectives of this work is to simulate the growth step in a much larger system than the one studied in our previous work (the crystallite we obtain in this work is more than five times larger than the one obtained in our preliminary study¹⁴). Our aim is to determine how the initial cross-nucleation event of a hcp cluster of the fcc nucleus affects the growth mechanism. Figure 2 indicates that the fcc and hcp polymorphs grow at the same rate, suggesting that both polymorphs play the same role during the growth of the crystallite. The snapshots at $t = 40$, 80, and 140 presented in Figure 3 provide a direct insight into the molecular mechanisms accounting for the growth of the nucleus. Growth proceeds through successive steps of cross-nucleation. After the initial cross-nucleation of a few hcp layers on the structurally compatible (111) plane of the fcc nucleus, the fcc polymorph cross-nucleates on the hcp layers before hcp cross-nucleates again on fcc and so on. These snapshots clearly demonstrate that just as the hcp polymorph cross-nucleates on the (111) planes of a mainly fcc crystallite, the fcc polymorph can cross-nucleate on the hcp polymorph. This finding confirms that cross-nucleation is essentially governed by kinetics since it is just as likely to have a metastable polymorph cross-nucleate on the stable polymorph than to have the stable polymorph cross-nucleate on a metastable polymorph. These two results are in excellent agreement with the experimental results of Yu and co-workers.⁹ Yu et al. observed the cross-nucleation of metastable polymorphs on a stable polymorph as well as the inverse. Yu et al. also showed that, in both cases, the new

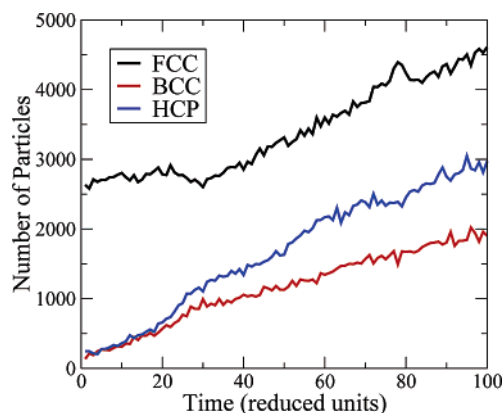


Figure 4. Evolution of the number of fcc-like, bcc-like, and hcp-like particles during the growth from the (111) plane of a fcc lattice.

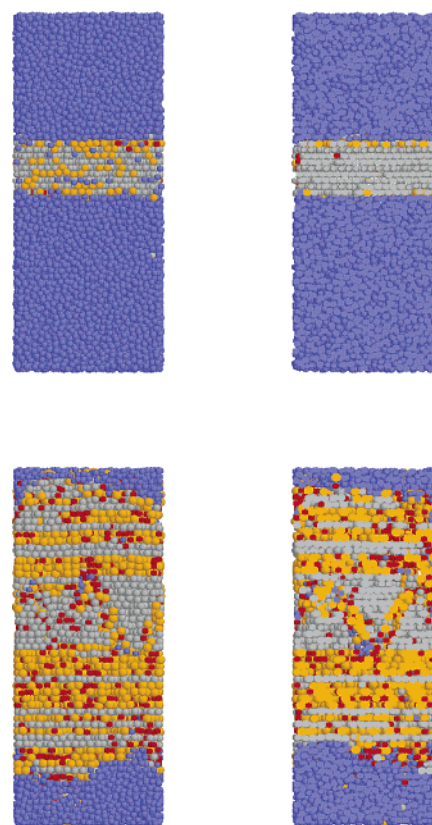


Figure 5. Growth from the (111) plane of a fcc crystal. Top: Outside view and cross-section at $t = 0$. Bottom: Outside view and cross-section at $t = 100$ (blue: liquid-like particles; gray: fcc-like particles; yellow: hcp-like particles; and red: bcc-like particles).

polymorph formed grew faster than (or at least as fast as, as seen in our case) the one initially present. The succession of cross-nucleations reported in this work has not been observed experimentally so far. We attribute its occurrence for the Lennard-Jones system to the fact that the two polymorphs, hcp and fcc, grow at a similar rate.

Finally, we turn to the study of the crystal growth from the (111) face of a Lennard-Jones crystal into the melt (the conditions of temperature $T = 0.86$ and pressure $P = 5.68$ are exactly the same as before). We only present the results obtained for one of the MD trajectory (all 10 MD trajectories exhibit the same behavior). We plot the evolution of the number of fcc (N_{fcc}), hcp (N_{hcp}), and bcc (N_{bcc}) particles during the growth in Figure 4. We also provide snapshots of the system at the beginning and at the end of the MD trajectory in Figure 5. We

recall that until $t = 0$, the system, with the exception of 9 layers of fcc particles, is equilibrated at $T = 1.5$ and $P = 5.68$. $t = 0$ denotes the time at which we set $T = 0.86$ and let the whole system evolve freely. As shown in Figure 5, at $t = 0$, the crystalline part of the system consists of the layers of fcc particles with a few hcp and bcc defects (N_{hcp} and N_{bcc} are roughly the same for $0 < t < 10$).

The growth mechanism we observe from the (111) face into the melt is the same as the one observed for the growth of a crystallite resulting from a homogeneous nucleation event. We observe in Figure 4 the same sequence as in Figure 2. At $t = 20$, N_{hcp} starts to grow at a much faster rate than N_{bcc} . For longer times $t > 30$, N_{hcp} and N_{fcc} grow at a similar rate. Figure 5 confirms that growth from the (111) face proceeds along the same mechanism at the molecular level. Indeed, at the end of the MD trajectory, we observe the same pattern as in Figure 3 resulting from the successive cross-nucleations of layers of the metastable polymorph hcp on the stable polymorph fcc and of layers of fcc on hcp. This is yet another proof that cross-nucleation takes place in the Lennard-Jones system and that cross-nucleation is a kinetic phenomenon. This also proves that the technique used experimentally to control polymorphism, i.e., seeding by a crystal of the stable polymorph (fcc in the case of the Lennard-Jones system), will not prevent the formation of the hcp polymorph.

4. Conclusion

The simulations presented in this work demonstrate that cross-nucleation takes place during the crystallization of a supercooled Lennard-Jones liquid as well as during the crystal growth from the (111) face of a perfect fcc crystal into the melt. Our results show that, in both cases, crystal growth proceeds through successive steps of cross-nucleation either of a metastable polymorph on the stable polymorph or of the stable polymorph on a metastable polymorph. Our findings are in excellent agreement with the experimental results on cross-nucleation.⁹ We find that cross-nucleation is mostly governed by kinetics. First, we observe that the cross-nucleation of a metastable polymorph (hcp) on a crystal of the stable polymorph occurs as often as the inverse. Second, we find that the two polymorphs (fcc and hcp) grow at the same rate. Our results also show that cross-nucleation is selective since we did not observe the cross-nucleation of the bcc polymorph. This is in accord with the fact that cross-nucleation between some polymorphs cannot be

observed experimentally.⁹ Cross-nucleation had only been observed in a few systems so far.^{7–9} Our simulations³⁰ demonstrate that cross-nucleation also occurs in a system of spherical particles, which suggests that this phenomenon is likely to play an important role in many polymorphic systems of technological interest.

References and Notes

- (1) Bernstein, J. *Polymorphism in Molecular Crystals*; Oxford University Press: Oxford, UK, 2002.
- (2) Dunitz, J.; Bernstein, J. *Acc. Chem. Res.* **1995**, *28*, 193.
- (3) Bauer, J.; Spanton, S.; Henry, R.; Quick, J.; Dziki, W.; Porter, W.; Morris, J. *Pharm. Res.* **2001**, *18*, 859.
- (4) Bernstein, J.; Davey, R. J.; Henck, J.-O. *Angew. Chem., Int. Ed.* **1999**, *38*, 3441.
- (5) ter Horst, J. H.; Kramer, H. J. M.; Jansens, P. J. *Cryst. Growth Des.* **2002**, *2*, 351.
- (6) Blagden, N.; Davey, R. J. *Cryst. Growth Des.* **2003**, *3*, 873.
- (7) Yu, L. *J. Am. Chem. Soc.* **2003**, *125*, 6380.
- (8) Stoica, C.; Tinnemans, P.; Meekes, H.; Vlieg, E. *Cryst. Growth Des.* **2005**, *5*, 975.
- (9) Chen, S.; Xi, H.; Yu, L. *J. Am. Chem. Soc.* **2005**, *127*, 17439.
- (10) Tao, J.; Yu, L. *J. Phys. Chem. B* **2006**, *110*, 7098.
- (11) Huang, J.; Chen, S.; Guzei, I. A.; Yu, L. *J. Am. Chem. Soc.* **2006**, *128*, 11985.
- (12) Ostwald, W. Z. *Phys. Chem.* **1897**, *22*, 289.
- (13) Cardew, P. T.; Davey, R. J. *Faraday Soc. Discuss.* **1993**, *95*, 160.
- (14) Desgranges, C.; Delhommelle, J. *J. Am. Chem. Soc.* **2006**, *128*, 10368.
- (15) van der Hoef, M. A. *J. Chem. Phys.* **2000**, *113*, 8142.
- (16) Choi, Y.; Ree, T.; Ree, F. H. *Phys. Rev. B* **1993**, *48*, 2988.
- (17) Somasi, S.; Khomani, B.; Lovett, R. *J. Chem. Phys.* **2000**, *113*, 4320.
- (18) Allen, M. P.; Tildesley, D. J. *Computer Simulations of Liquids*; Oxford University Press: Oxford, UK, 1987.
- (19) Torrie, G. M.; Valleau, J. P. *Chem. Phys. Lett.* **1974**, *28*, 578.
- (20) van Duijneveldt, J. S.; Frenkel, D. *J. Chem. Phys.* **1992**, *96*, 4655.
- (21) ten Wolde, P. R.; Ruiz-Montero, M. J.; Frenkel, D. *Phys. Rev. Lett.* **1995**, *75*, 2714.
- (22) ten Wolde, P. R.; Ruiz-Montero, M. J.; Frenkel, D. *J. Chem. Phys.* **1996**, *104*, 9932.
- (23) Auer, S.; Frenkel, D. *Nature* **2001**, *409*, 1020.
- (24) Steinhardt, P. J.; Nelson, D. R.; Ronchetti, M. *Phys. Rev. B* **1983**, *28*, 784.
- (25) Trudu, F.; Donadio, D.; Parrinello, M. *Phys. Rev. Lett.* **2006**, *97*, 105701.
- (26) Moroni, D.; ten Wolde, P. R.; Bolhuis, P. G. *Phys. Rev. Lett.* **2005**, *94*, 235703.
- (27) Burke, E.; Broughton, J. Q.; Gilmer, G. H. *J. Chem. Phys.* **1988**, *89*, 1030.
- (28) Gulam, Razul, M. S.; Hendry, J. G.; Kusalik, P. G. *J. Chem. Phys.* **2005**, *123*, 204722.
- (29) Cacciuto, A.; Auer, S.; Frenkel, D. *Nature* **2004**, *428*, 404.
- (30) Desgranges, C.; Delhommelle, J. *J. Am. Chem. Soc.* **2006**, *128*, 15104.